

Classification of Multiscaling in Fracture and Fragmentation

A. Bershadskii^{1, 2} and Emily S. C. Ching¹

Received August 23, 1999; revised January 8, 2001

We propose a method to classify multifractal properties, which have been found in many systems. We then study the multifractal properties previously found in various models of fracture and fragmentation, and show explicitly that they indeed fall into the two classes proposed in our method. Several interesting features are also revealed.

KEY WORDS: Scaling; multifractality; fracture; fragmentation.

1. INTRODUCTION

In the last decade, the scaling properties of fracture and the related fragmentation processes have been actively investigated (see, for instance, ref. 1 and references therein). Multifractality has been found in various simple models of fracture of disordered media just before the breakdown of the system and in fragmentation after the system breaks.

One of the most successful approaches to model fracture of disordered materials is to represent a continuous material by a lattice of bonds. In the simplest models, the vectorial force and displacement are replaced respectively by the scalar current and voltage passing through and across the bond. Disorder has been introduced in different ways in different models. In the random resistor network model,⁽²⁾ each bond is assigned as a conductor carrying a unit resistance with probability ψ or an insulator with probability $1 - \psi$. For large ψ , the system will remain conducting or intact

¹ Department of Physics, The Chinese University of Hong Kong, Shatin, N.T., Hong Kong.

² Present and permanent address: Machanaim Center, P.O. Box 39953, Ramat-Aviv 61398, Tel-Aviv, Israel.

as a whole. When ψ is less than some percolation threshold, the system breaks down or ruptures, becoming insulating. In the fuse model,⁽³⁾ all the bonds in the lattice are originally identical resistors or fuses. A bond or resistor will break or burn when the current passing through it is larger than some threshold value and the threshold currents are randomly drawn from some continuous distribution. As the external strain or voltage is increased, the bonds will break one by one until the whole network fails, that is, becomes insulating.

In the central force model,⁽³⁾ the vectorial nature of fracture is reinstated in which the material is represented by a network of Hookean springs. The springs can freely rotate around the nodes of the lattice and will break when they are elongated or compressed beyond a certain threshold. The threshold forces are again drawn from some continuous distribution. No bending effects are taken into account in this model. With an imposed external strain, the springs will break one by one until the whole system fails as in the scalar fuse model.

Several models have been introduced to study fragmentation numerically. In these models, an object is described by an assembly of basic constituents or building blocks which are either connected to each other via elastic springs or beams,^(4, 5) or interact with each other via some force potential.^(6, 7) The object is then subjected to some external force^(4, 5) or the constituents be given some specified initial velocities which mimic the effect of the impact forces^(6, 7) and the whole system evolves according to Newtonian dynamics. The connection or bond between the constituents is taken to be broken when some specific rules are satisfied.

Multifractal properties have been found in both fracture models at the point of breakdown^(2, 3) and fragmentation models.^(5, 7) The scaling properties of the distribution of the fluctuating quantities of interest, say the voltage and current distributions in the random resistor network and the mass distribution of the fragments in the fragmentation models, have to be characterized by a set of exponents. That is, the scaling exponents of the moments of the distribution are not simply proportional to the order of the moments.

In this paper, we propose a method to classify multifractality according to the functional dependence of the exponents on the order of the moment. Then we use this method to study the multifractal properties of the various models of fracture and fragmentation. Several interesting features have been found.

2. CLASSIFICATION OF MULTIFRACTALITY

Suppose the distribution of a certain fluctuating quantity of interest X is multifractal. To characterize the multifractality, one studies the moments

of this quantity $\langle X^p \rangle$, where p is the order of the moments. These moments scale with some parameter a :

$$\langle X^p \rangle \sim a^{\chi(p)} \quad (1)$$

with exponents $\chi(p)$. For example, in the random resistor network model, the moments of the voltage distribution scale with the size of the network.⁽²⁾ The distribution is multifractal in that the exponents $\chi(p)$ are not simply proportional to p .

It is known that in the thermodynamic interpretation of multifractality,^(8, 9) p can be interpreted as the inverse of temperature. That is, $p \sim T^{-1}$. Therefore, it is interesting to check whether $\chi(p)$ does indeed exhibit a phase-transition-like behavior:

$$\chi(p) \sim (p - p_c)^\gamma \quad (2)$$

in the vicinity of some critical point p_c . Equation (2) has been shown to hold for the multifractal properties observed in a wide variety of systems including random walk on linear fractals, diffusion limited aggregation, and turbulence.⁽¹⁰⁾ In this paper, we shall show explicitly that Eq. (2) also holds for the multifractal properties found in the models of fracture and fragmentation discussed in Section 1.

One can use Eq. (2) to classify multifractality depending on whether the critical point p_c is zero or not. The case of a finite non-zero p_c corresponds to the usual critical phenomena with a finite critical temperature T_c . Since p is a dimensionless parameter, it is natural to normalize temperature T by T_c to get $p_c = 1$. The other class is $p_c = 0$, which corresponds to an infinite critical temperature. This can be taken as a transition from a state of negative temperature to another state of positive temperature (see, for instance, ref. 11).

Hence, we can classify multifractal properties into the following two different types:

$$\chi(p) \sim (p - 1)^\gamma \quad (3)$$

in the vicinity of the critical point $p_c = 1$, and

$$\chi(p) \sim p^\gamma \quad (4)$$

In the following, we shall use this method to study the multifractal properties found in the various models of fracture and fragmentation.

3. MULTIFRACTALITY AT THE POINT OF BREAKDOWN

The local strain or stress distribution just before the system breaks has been found to possess multifractality. For a random resistor network, the point of breakdown is naturally the percolation threshold. The local strain distribution is given by the voltage distribution in the bonds of the network. The moments of the voltage distribution are given by

$$\langle V^p \rangle = \sum \frac{n(V)}{N_0} V^p, \quad (5)$$

where $n(V)$ is the number of bonds with a voltage drop V and N_0 is the total number of conducting bonds.

At the percolation threshold, the moments $\langle V^p \rangle$ were found⁽²⁾ to scale with L , the size of the network:

$$\langle V^p \rangle \sim L^{-\chi(p)} \quad (6)$$

and the exponents $\chi(p)$ are a nonlinear function of p . This nonlinearity clearly demonstrates that the voltage distribution is multifractal.

On the other hand, for the fuse and the central force models, the point of breakdown is the point when the last bond or spring is cut before the whole system falls apart. The local stress distribution is given by the local current distribution in the fuse model or the local forces distribution in the central force model. The moments of these two distributions are given respectively by

$$\langle i^p \rangle = \sum \frac{n(i)}{N_0} i^p \quad (7)$$

and

$$\langle f^p \rangle = \sum \frac{n(f)}{N_0} f^p \quad (8)$$

where N_0 is the total number of conducting bonds or intact springs. The moments were also found to scale with the size of the lattice L , with exponents that are again not simply proportional to p .⁽³⁾

To check whether the multifractal properties found in these models can be classified using our method proposed in Section 2, we show the log-log plots of $\chi(p)$ vs p and $p-1$ respectively for the three models in Fig. 1. Data for the random resistor network model are taken from ref. 12

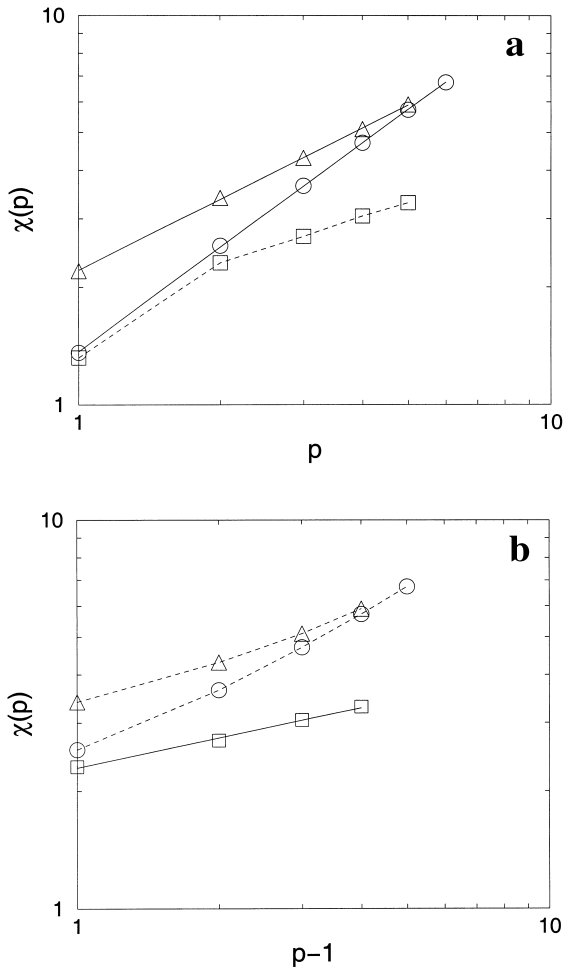


Fig. 1. (a) $\chi(p)$ vs p and (b) $\chi(p)$ vs $p-1$ in log-log plots for the three models: Random resistor network at the percolation threshold (circles), scalar fuse model (squares), and vector central force model (triangles). The solid lines, which are best fits to the data points, show that $\chi(p) \sim p^\gamma$ for the random resistor network model and the central force model but $\chi(p) \sim (p-1)^\gamma$ instead for the fuse model. The dashed lines, joining the data points, are guides to the eye.

and those for the fuse and central force models are taken from ref. 13. The number of data points is small and the data extend over less than a decade. Nevertheless, we can see that $\chi(p)$ for the random resistor network and the vector central force model are well described by Eq. (4) for $p \geq 1$ while that for the scalar fuse model has to be described by Eq. (3) for $p \geq 2$. Thus, the

dependence of $\chi(p)$ on p in these models indeed falls into the two classes proposed in our method.

Interestingly, the multifractality of the voltage distribution in the random resistor network belongs to the class described by (4) with $\gamma \approx 0.89$ while that of the current distribution in the fuse model belongs to the other class described by (3) with $\gamma \approx 0.26$. This result, therefore, suggests that the nature of the multifractal properties of local strain or stress depends on the details of how the system gets to the point of breakdown. For the central force model, $\chi(p)$ is better described by (4) than by (3) even though the system gets to the point of breakdown in a similar fashion as that of the fuse model. This, therefore, suggests that the nature of the multifractality of the local stress distribution also depends on the vectorial character of the stress field.

4. MULTIFRACTALITY AFTER BREAKDOWN

In the previous sections, we have studied the statistical properties of the local stress or strain distribution just before the breakdown of the system. One would expect that multifractality of this distribution would result in multifractality of the fragments distribution after the system breaks down (cf. ref. 14). This has indeed been found.^(5, 7)

Fragmentation in collision of solids was numerically simulated using a two-dimensional dynamical model of granular solids.⁽⁵⁾ In this model, the solid consists of unbreakable and undeformable grains that are connected by elastic beams which can be broken according to a rule that takes into account of stretching and bending of the connections.

In another numerical model of fragmentation,⁽⁷⁾ the two-dimensional object consists of N particles, which interact with each other pairwise via the Lennard-Jones potential. The effect of the fragmentation-induced forces is represented by assigning the particles some specified initial velocities. The fragmentation process is followed using molecular dynamics calculations.⁽¹⁵⁾ Each particle moves according to Newton's laws of motion. As time evolves, the particles distribute themselves in clusters or fragments of various sizes.

In both models, the fragment mass distribution was found to depend on the input energy which is expressed in terms of a dimensionless parameter R . In ref. 5, R was taken as the square root of the ratio of the collision and the binding energies while in ref. 7, R is the ratio of the initial kinetic energy to the absolute value of the initial potential energy of the particles.

The moments of the mass distribution

$$\langle m^p \rangle = \sum \frac{n(m)}{N} m^p \quad (9)$$

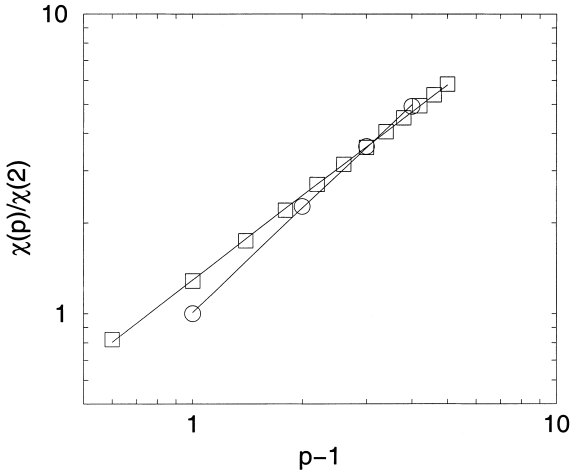


Fig. 2. $\chi(p)/\chi(2)$ vs $(p-1)$ in a log-log plot for the mass distribution of fragments in the two fragmentation models: grain-beam model (circles) and Lennard-Jones-particle model (squares). The straight lines, which are the least-square fit to the data points, indicate that $\chi(p) \sim (p-1)^\gamma$ for both models.

where $n(m)$ is the number of fragments with mass m and N is the total number of fragments, scale with R as

$$\langle m^p \rangle \sim R^{\chi(p)} \quad (10)$$

The exponents $\chi(p)$ are again not simply proportional to p showing that the mass distribution is multifractal.^(5, 16)

In Fig. 2, we plot $\chi(p)$ vs p for the two fragmentation models.⁽¹⁷⁾ We see that $\chi(p) \sim (p-1)^\gamma$ for both models with $\gamma \approx 1.15$ for the grain-beam model and $\gamma \approx 0.93$ for the Lennard-Jones-particle model. Thus, although the specific details of the models differ, the multifractality of the fragment mass distribution belongs to the same class. Moreover, this multifractality of the fragment mass distribution after the breakdown of the system belongs to the same class as that of the local current distribution in the scalar fuse model just before the breakdown of the system.

5. SUMMARY

For any system in which the distribution of the quantity of interest exhibits multifractal properties, we have shown how to classify the multifractality according to the functional dependence of the scaling exponents

$\chi(p)$ of the moments of the distribution on the order p . Using the thermodynamic interpretation of multifractality, this classification can be associated with a phase-transition-like behavior of $\chi(p)$ at either a finite or an infinite critical temperature. We have then used this method to study the multifractality previously found in several models of fracture and fragmentation. We have shown explicitly that the multifractal properties found in these models indeed fall into the two classes proposed in our method. Some interesting features have also been revealed. We have found that the multifractality of the local strain or stress distribution in the random resistor network at the percolation threshold is different from that of the fuse model at the point when the last bond is cut before the whole system fails. Hence, the nature of the multifractal properties of the local strain or stress distribution, which is expected to contain useful information of the regions that are responsible for the final breakdown of the system, depends on how the system gets to the point of breakdown. The multifractal properties also depend on the vectorial nature of the stress field. Moreover, multifractality of the system just before breakdown leads to similar multifractality in the system after breakdown as expected. Further understanding the physical significance of the two classes of multifractality and the value of γ will be an interesting problem for future investigations.

ACKNOWLEDGMENTS

This work is supported by the Hong Kong Research Grants Council (Grant 315/96P). The authors are grateful to J. Fineberg, F. Kun, and D. Stauffer for correspondence, and to N. Schörghofer and anonymous referees for comments and suggestions.

REFERENCES

1. H. J. Herrmann and S. Roux, eds., *Statistical Models for the Fracture of Disordered Media* (North Holland, Amsterdam, 1990).
2. L. de Arcangelis, S. Redner, and A. Coniglio, *Phys. Rev. B* **31**:4725 (1985).
3. L. de Arcangelis, A. Hansen, H. J. Herrmann, and S. Roux, *Phys. Rev. B* **40**:877 (1989).
4. Y. Hayakawa, *Phys. Rev. B* **53**:14828 (1996).
5. F. Kun and H. J. Herrmann, *Phys. Rev. E* **59**:2623 (1999).
6. U. Naftaly, M. Schwartz, A. Aharony, and D. Stauffer, *J. Phys. A* **24**:L1175 (1991).
7. E. S. C. Ching, Y. Y. Yiu, and K. F. Lo, *Physica A* **265**:119 (1999).
8. H. E. Stanley and P. Meakin, *Nature* **335**:405 (1988).
9. A. Arneodo, E. Bacry, and J. F. Muzy, *Physica A* **213**:232 (1995).
10. A. Bershadskii, *Physica A* **268**:142 (1999).
11. L. D. Landau and E. M. Lifshitz, *Statistical Physics*, Part 1 (Pergamon Press, 1980).

12. L. de Arcangelis, S. Redner, and A. Coniglio, *Phys. Rev. B* **34**:4656 (1986).
13. L. de Arcangelis, in *Statistical Models for the Fracture of Disordered Media*, H. J. Herrmann and S. Roux, eds. (North Holland, Amsterdam, 1990), p. 229.
14. E. Sharon and J. Fineberg, *Phys. Rev. B* **54**:7128 (1996).
15. B. L. Holian and D. E. Grady, *Phys. Rev. Lett.* **60**:1355 (1988).
16. E. S. C. Ching, *Physica A* **288**:403 (2000).
17. Data for the grain-beam model were obtained from F. Kun, private communication.